Journal of Informatics and Web Engineering

Vol. 2 No. 1 (March 2023) eISSN: 2821-370X

Robust Image Watermarking With Quaternion Fractional-Order Polar Harmonic-Fourier Moments Based On Wavelet Transformation: Resistance Against Rotation Attacks

Wang Jing[1*], Ling Weay Ang[2], Sellappan Palaniappan[3] and Bing He[4]

[1,2,3] Malaysia University of Science and Technology, Petaling Jaya. 47810, Malaysia

[1,4]Weinan Normal University, Weinan. 714000, China

**corresponding author: (wang.jing@phd.must.edu.my)*

Abstract - This study presents a zero-watermarking algorithm that can resist rotation attacks. The algorithm uses quaternion fractional-order polar harmonic-Fourier moments (QFr-PHFMs) based on wavelet-transformation. First, the wavelet-transformation is applied to each component of the host image, which is in RGB three-channel color. The low-frequency sub-bands of each component are then extracted and represented using quaternion algebra. Multiple QFr-PHFMs are calculated, and the invariants of the QFr-PHFMs are utilized to establish the watermark system. The watermark extraction process is also simplified. The detection of the image requires a two-level wavelet transformation, followed by the calculation of multiple invariant moments of the low-frequency sub-image. The experimental results are shown and compared with similar methods. Simulations show that this method can produce high-quality visual effects and withstand noise, filtering, JPEG compression, and cropping attacks.

Keywords — Zero Watermarking, Quaternion Fractional-Order Polar Harmonic-Fourier Moments, Wavelet Transform, Invariant Moments

Received: 14 December 2022; Accepted: 23 February 2023; Published: 16 March 2023

I. INTRODUCTION

In recent years, the field of network information security has gained significant attention due to the rapid advancement of multimedia and information network technology. Digital picture watermarking is recognized as an effective way of addressing information security and copyright protection issues [1-2]. By adding watermarks to the original data, traditional digital watermarking establishes the ownership of multimedia creations. Most of these techniques achieve their goal of embedding the watermark information by altering the image's spatial or frequency domain information[3-4]. The encoded watermark information is then altered to prevent tampering. While some researchers have proposed the use of visual masks based on the human visual system (HVS), this approach complicates the embedding and extraction of watermarks and increases computational cost, making it unfeasible for practical applications. Furthermore, this method is not secure as a malicious user who understands the visual mask can still detect the presence of the watermark using professional detection software and remove it, reducing the overall security of the digital watermark.

The recent advancements in zero-watermarking technology have effectively addressed the limitations of conventional watermarking algorithms. Unlike traditional methods, zero-watermarking technology does not modify the original multimedia data, instead, it leverages the unique features of the data to embed the watermark information, resulting in

Journal of Informatics and Web Engineering
https://doi.org/10.33093/jiwe.2023.2.1.6

Published by MMU Press. URL: https://journals.mmupress.com/jiwe

increased robustness and security. The concept of zero digital watermarking was first proposed by Wen et al. as a way to resolve the trade-off between watermark robustness and imperceptibility [5]. The zero-digital watermarking approach uses the inherent properties of the carrier media to create a distinctive watermark, thereby enabling copyright protection without modifying the original work. However, zero-digital watermarking relies on establishing an intellectual property right as proof of data copyright authentication.

Following Wen's work, zero-watermarking technology has gained significant attention, and various research results and papers have been published [6]. However, most existing methods [7] are limited to non-geometric attacks, such as noise, lossy compression, filtering, and cropping, and are less effective against geometric attacks such as rotation, scaling, and translation. This paper proposes a color digital image zero-watermarking approach in the wavelet transform domain, which is resistant to rotation attacks. The suggested QFr-PHFMs are robust against rotation attacks and have a high degree of resistance to noise, lossy compression, filtering, cropping, and other attacks.

II. RELATED WORK

Orthogonal moments, especially those of orthogonal nature, have proven to be effective for image description in image feature extraction. Their independent orders and low sensitivity to noise have drawn attention from researchers in image processing and pattern recognition. The concept of orthogonal image moments was first discussed in the early 1980s, and they can be separated into Cartesian and circularly orthogonal moments. Circularly orthogonal moments, including Zernike moments [8], Bessel-Fourier moments [9], and Legendre-Fourier moments [10], are rotationally invariant and hence the focus of research. However, traditional orthogonal moments have limitations, as their orders can only be integers, reducing their description and anti-noise capabilities.

Fractional-order orthogonal moments (Fr-OMs) are a recent innovation that extends the use of integer-order orthogonal polynomials to fractional-order. Xiao et al. introduced two types of Fr-OMs defined in Cartesian and polar coordinates using Legendre polynomials [11]. Zhang et al. proposed fractional orthogonal Fourier-Mellin moments for binary image pattern recognition [12]. Quaternions, as a mathematical tool, can be used to deal with color images as a whole and have been applied in various domains such as image reconstruction, pattern identification, and digital image watermarking. For example, Wang et al. used quaternion algebra to develop the quaternion polar complex exponential transform (QPCET) [13] and Chen et al. proposed quaternion Zernike moments (QZMs) for color images, investigating their invariance to rotations, scaling, and translations (RST) [14]. Shao et al. introduced the quaternion Bessel-Fourier moments (QBFM) and evaluated the value of phase information [15]. However, the application of quaternions and fractional-order picture moments in digital watermarking, especially in the domain of zero-watermarked color photographs in the transform domain, has not been widely explored in the literature.

This study presents a new zero-watermarking approach to counter rotation attacks. The approach is based on the use of quaternion fractional-order polar harmonic Fourier moments in the wavelet transform domain. The primary contributions of the paper are as follows: (1) A theoretical framework for the derivation of quaternion fractional-order polar harmonic Fourier moments (QFr-PHFMs) and the demonstration of rotation invariance in orthogonal polar coordinates with geometric rotation invariance. (2) The development of a novel framework for zero-watermark registration and watermark detection, which utilizes QFr-PHFMs and wavelet transforms. (3) The conduct of simulation experiments to validate the proposed theoretical algorithm.

III. WAVELET TRANSFORM

The wavelet analysis, also referred to as the time-scale analysis method, is a new technique in time-frequency analysis that has evolved from Fourier analysis. It is recognized for its multi-scale analytical properties and ability to provide good localization qualities in both time and frequency domains. This is consistent with computer vision and human vision characteristics. In 1988, Mallet introduced wavelet transform theory to signal processing and proposed scaling analysis methodologies. He also presented an algorithm for decomposing a two-dimensional image into different frequency channels and for reconstructing images using decomposed features.

The discrete wavelet transform of an image signal can be seen as higher and lower pass filtering of the two-dimensional signal's columns and rows, equivalent to a four-channel filter operation [16]. The two-dimensional signal can then be retrieved from subbands LL1, LH1, HL1, and HH1. The transform coefficients on the subbands can be continuously decomposed until the desired series is obtained. The lowest frequency coefficient, which contains the majority of the energy of the original image, has the largest absolute value. Figure 1 depicts the process of three-level wavelet decomposition. Hence, the wavelet analysis allows the extraction of low-frequency coefficients and related calculations. In this study, the Haar wavelet basis function is used to implement the discrete wavelet transform. The Matlab code implementation is as follows: [LL1, HL1, LH1, HH1]=dwt2 (I, "haar"), where I represents the original picture and LL1, HL1, LH1, and HH1 represent the low-frequency sub-band image, horizontal detail sub-band image, vertical detail sub-band image, and diagonal detail sub-band image, respectively.

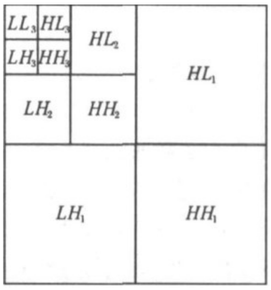

Figure 1. The diagram of three-level wavelet decomposition

IV. QFR-PHFMS

If $f^c(x,y)$ denotes an RGB image in RGB color space ; then, the color image represented by quaternion is as follows:

$$f^c(x,y) = f_r(x,y)i + f_g(x,y)j + f_b(x,y)k \tag{1}$$

Where $f_r(x,y)$, $f_g(x,y)$, and $f_b(x,y)$ are respectively the red, green, and blue components of a color image, and i , j and k are unit imaginary numbers.

Subsequently, the proposed real-order (fractional-order) polar harmonic-Fourier moments (Fr-PHFMs) can be defined as:

$$p_{nm}^{\alpha} = \frac{2}{\pi}\int_0^{2\pi}\int_0^1 f(r,\theta)\left[R_n^{\alpha}(r)\exp(im\theta)\right]^* rdrd\theta \tag{2}$$

Where $f(r,\theta)$ represents a grayscale image in polar coordinates, and $R_n^{\alpha}(r)\exp(im\theta)$ with real number $\alpha > 0$ is the kernel functions of Fr-PHFMs, and the radial basis functions (RBFs) $R_n^{\alpha}(r)$ are given below：

$$R_n^{\alpha}(r) = \begin{cases} \frac{1}{\sqrt{2}}\sqrt{\alpha}r^{\alpha-1} & n = 0 \\ \sqrt{\alpha}r^{\alpha-1}\sin((n+1)\pi r^{2\alpha}) & n = odd \\ \sqrt{\alpha}r^{\alpha-1}\cos(n\pi r^{2\alpha}) & n = even \end{cases} \tag{3}$$

Then, the QFr-PHFMs for the original color image can be expressed as follows:

$$M_{nm}^{\alpha} = \frac{2}{\pi}\int_0^{2\pi}\int_0^1 f^c(r,\theta)R_n^{\alpha}(r)\exp(-\mu m\theta)rdrd\theta \tag{4}$$

According to Equation(4), the QFr-PHFMs has rotation invariance inherently, and the proof process mainly includes the following steps: Firstly, let the rotated color image be $f^q(r,\theta+\varphi)$, and φ is the angle of rotation. Then, the QFr-PHFMs of the rotated color image are described as follows:

$$M_{nm}^{\alpha}(I^r) = \frac{1}{2\pi}\int_0^{2\pi}\int_0^{\infty} f^q(r,\theta+\varphi)R_n^{\alpha}(r)\exp(-\mu m\theta)rdrd\theta \tag{5}$$

By letting $\theta' = \theta + \varphi$, we have $\theta = \theta' - \varphi$ and $d\theta = d\theta'$. Equation (5) can be rewritten as:

$$M_{nm}^{\alpha}(I^r) = \frac{1}{2\pi}\int_0^{2\pi}\int_0^{\infty} f^q(r,\theta+\varphi)R_n^{\alpha}(r)\exp(-\mu m\theta)rdrd\theta$$

$$=[\frac{1}{2\pi}\int_0^{2\pi}\int_0^{\infty} f^q(r,\theta')R_n^{\alpha}(r)\exp(-\mu m\theta')rdrd\theta']\exp(\mu m\varphi) \quad (6)$$
$$= M_{nm}^{\alpha}(I)\exp(\mu m\varphi)$$

Taking the module on both sides of Equation (6), we have

$$|M_{nm}^{\alpha}(I^r)|=|M_{nm}^{\alpha}(I)| \quad (7)$$

V. PROPOSED ZERO-DIGITAL IMAGE WATERMARKING METHODOLOGY

This study introduces a new method of zero watermarking that uses QFr-PHFMs to overcome the challenge of geometric transformations in traditional digital watermarking. In this approach, color photos are watermarked with the proposed QFr-PHFMs. Traditional image processing techniques, such as adding noise, compressing the image, and smoothing the image, can effectively resist traditional 2D watermarking methods. However, these techniques cannot solve the problem of image distortion caused by geometric transformations. To address this issue, the study proposes using wavelet transforms and QFr-PHFMs to create a zero watermarking technique that is resilient to geometric transformation operations.

A. The registration stage of zero-watermarking methodology

Figure 2 shows the registration implementation of our proposed zero-watermarking method.

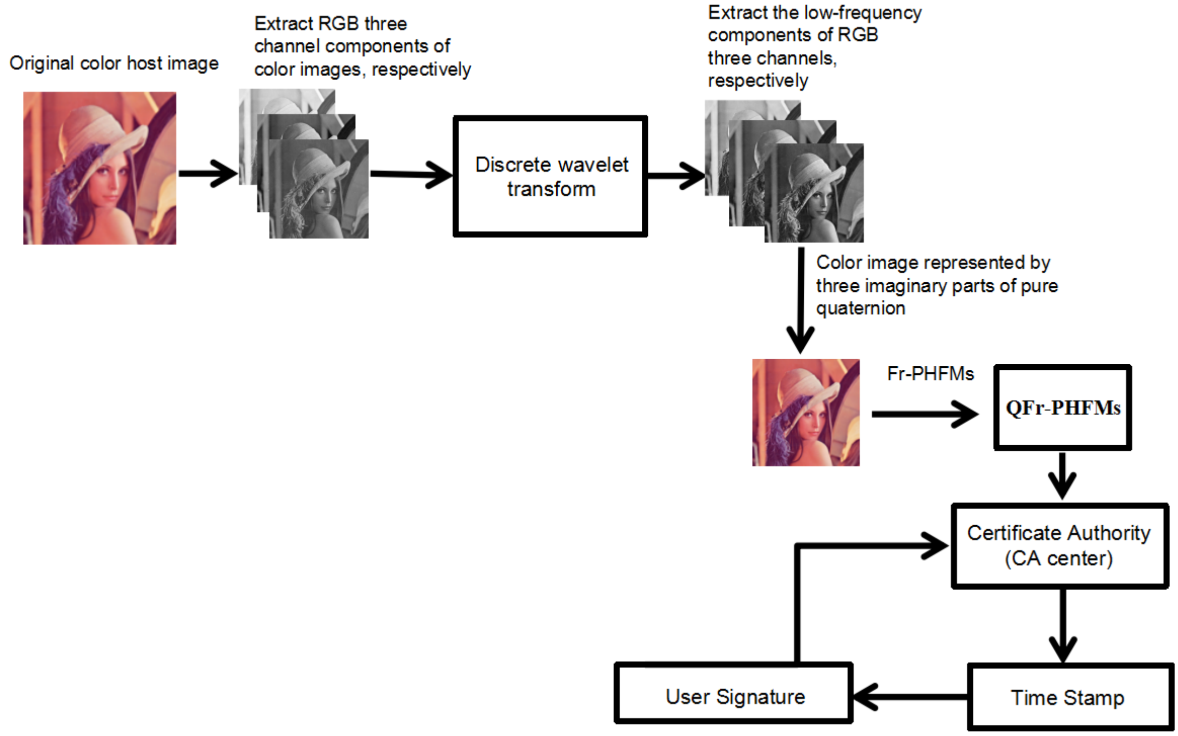

Figure 2. Watermark registration scheme

The algorithm proceeds by the following steps:

Step 1: This study involves obtaining the R, G, and B channel components from the original color host image and then performing a two-dimensional wavelet transformation on each component. The low-frequency components of the RGB channels are then extracted. Finally, the three low-frequency components are represented as a complete vector using three imaginary parts of a pure quaternion, resulting in a quaternion representation of a color image.

Step 2: A few of lower-order image moments' features of the designed QFr-PHFMs are extracted, which can be regarded as the one-dimensional vector $H_k^{(RGB)}$, $k = 1,2\ldots 25$. Here we set $H_k^{(RGB)} = \{h_{nm}^{(1)}, h_{nm}^{(2)}, \ldots h_{nm}^{(k)}, k = 25\}$, h_{nm}^{k} represents the lower-order image moments' features of $M_{nm}^{(\alpha)}$ in Equation (4). Then, the one-dimensional vector is registered in the copyright protection certificate authority center.

Step 3: The watermark information and the user's signature information are registered in the CA center in the order of registration time. Then, the host image is declared to be protected by copyright.

B. The detection stage of zero-watermarking methodology

Step 1: This part of the study explains the process of scaling and normalizing the color host image. Scaling normalization helps to standardize the size and range of the color image, making it easier to work with in further processing steps. There are two common methods for scaling normalization: (1) mapping the color image to a square region in cartesian coordinates with values ranging from 0 to 1, or (2) scaling the size of the color image to a fixed template while performing interpolation procedures. In this study, the image was normalized using the second method. The normalization process involved adjusting the size of the color image to a fixed template, while ensuring that the image quality was preserved during the interpolation procedure.
Let $\bar{f}^{(RGB)}(x, y)$, a colour image, serve as the final target image after scaling. Obtain $\bar{f}^{(RGB)}(x, y)$ by $\bar{\bar{f}}^{(RGB)}(x, y) = A_s[\bar{f}^{(RGB)}(x, y)]$, where $\bar{\bar{f}}^{(RGB)}(x, y)$ is a scaled image, and A_s is the transformation matrix shown in Equation (8).

$$A_s = \begin{bmatrix} \mu & 0 \\ 0 & \upsilon \end{bmatrix} \tag{8}$$

In this matrix, the parameters μ and υ represent the row and column scaling factors, respectively, of the image matrix. Image processing or pattern recognition also requires interpolation operations. Different interpolation approaches affect the visual quality of the scaled image. The MATLAB-based simulation environment adopts bilinear interpolation if $0.5 \le \mu, \upsilon \le 1$, and bicubic interpolation when $0 \le \mu, \upsilon \le 0.5$ or $\mu, \upsilon \ge 2$.

Step 2: This step performs the translations. First, the geometric moments $M_{pq}^{(RGB)}(x, y)$ are computed from the color image $\bar{\bar{f}}^{(RGB)}(x, y)$. These moments specify the coordinate position of the image's center of gravity: $x_a = x - \frac{M_{10}^{(RGB)}}{M_{00}^{(RGB)}}, y_a = y - \frac{M_{01}^{(RGB)}}{M_{00}^{(RGB)}}$. Image $\bar{\bar{f}}^{(RGB)}(x, y)$ is then translated to $\bar{\bar{f}}^{(RGB)}(x_a, y_a)$. Finally, the resulting centered color image is obtained.

Step 3: After processing the rotation, scaling, and translation steps, the color image is processed by steps 1 and 2 in the watermark registration scheme, thus obtaining a new feature vector $\tilde{H}_k^{(RGB)}$, $k = 1,2...25$.

Step 4: Extract one-dimensional vector $H_k^{(RGB)}$ from the CA copyright protection center, then, the absolute difference between the one-dimensional features $\tilde{H}_k^{(RGB)}$ and the one-dimensional features $H_k^{(RGB)}$ obtained in previous step is calculated, and subsequently the sum is accumulated .The specific calculation process is as in Equation (9).

$$d = \min\{ \frac{1}{cnf^2} \sum_{n=1}^{cnf} \sum_{m=1}^{cnf} | h_{nm}^{(k)} - \tilde{h}_{nm}^{(k)} | \} \tag{9}$$

In the paper, $cnf = 10$, $k = 1,2...25$. If $d \ge \varepsilon$ (here, the empirical threshold ε can be set in accordance with the particular experimental situation.) and the time stamp used for watermark registration does not accurately reflect the data given by the CA centre, the verification process is terminated. At this time, it has been established that the watermark data does not exist.

C. Simulation results and analysis

Figure 3. Original color host image

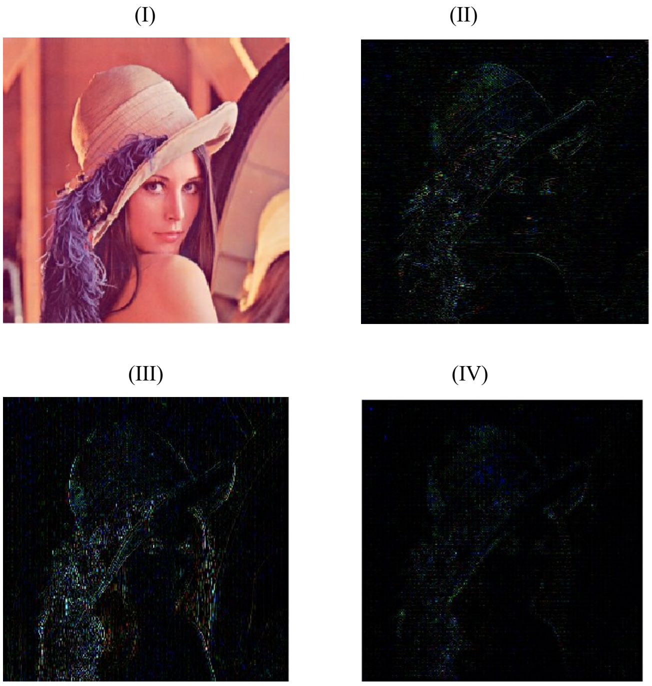

Figure 4. Wavelet decomposition (I) Low-frequency; (II)horizontal component; (III)Vertical component; (IV) Diagonal detail component

In the study, the Lena color image with the size 512×512 shown in Figure 3 is used as the host image to evaluate the proposed QFr-PHFMs-based zero-watermarking approach. The effect of two-dimensional wavelet transform in the above proposed algorithm is shown in Figure 4.The experiment is divided into two groups. The first experiment examines the stability of the proposed algorithm against various image processing attacks and the performance against powerful geometric operations like rotation, scaling, and translation. The second experiment checks the reliability of the algorithm by examining the false-alarm rate. The PSNR (peak signal-to-noise ratio)(see equation 10 and equation 11) is used to assess the quality of the original and attacked images, while equation 9 is used to evaluate the zero-watermarking performance. The closer the value is to zero, the better the performance. The simulations were run on a computer with an Intel(R) Core(TM) i5 processor with 2.50 GHz and 8 GB RAM running Windows 7 (64-bit).

$$MSE = \frac{1}{MN}\sum (I(x,y) - I'(x,y))^2 \qquad (10)$$

$$PSNR = 10l_g(255^2 / MSE) \qquad (11)$$

Here, $I(x,y)$ denotes original image and $I'(x,y)$ represents the attacked image.

Experiment 1: The researchers evaluated the performance of the proposed approach in handling noise interference and lossy compression in a color host image. The Lena color host image was infected with 25% Salt & Pepper noise and Gaussian noise with a variance of 0.04. The researchers mainly used median and mean filtering methods to treat the noise interference [19]. Additionally, the proposed approach was compared against two other algorithms, one based on direct grayscale and one on a single channel, in terms of performance verification tests for lossy compression. The results are shown in Table 1.

Table 1. Typical Results of Host Image Subjected to Non-geometric Transformations

Attacks	*PSNR*	*d*		
		Traditional direct grayscale method	Traditional single channel method	The proposed method
Salt & Peppers noise(Density: 25%)	13.28	0.00584	0.00632	0.00246
Gaussian noise (Parameter: 0.04)	12.51	0.0082	0.0039	0.00183
Median filtering (Size of window : 7)	23.31	0.00086	0.00045	0.00022
Smoothing filtering (Size of window: 5)	27.68	0.00022	0.00016	0.00011
Image compression (Parameter: 70%)	23.67	0.00042	0.00038	0.00019

The researchers also evaluated the performance of the proposed approach in handling geometric transformations, such as rotation, scaling, and translation, in the color host image. These transformations alter the pixel position in the image and make watermark identification more challenging. The researchers rotated the color image by 20°, 30°, and 90°, multiplied it by 0.7, 1.2, 1.8, and 2.5, and translated it according to the parameters listed in Table 2. The results showed that the proposed scheme outperformed other current schemes in overall performance.

Experiment 2: This experiment validated the proposed zero-watermarking scheme's false-alarm rate. The false-alarm rate in digital watermarking detects the number of unregistered images (that is, photos that have not been given copyright protection at the CA centre) that have been mistakenly detected based on the watermark information. To see if the proposed watermarking technique discovers unregistered photographs, 16 additional colour images from the standard image library were chosen. The images chosen were often used colour images in image processing, such as baboon, plane, and salt and pepper (see Figure 5 for all images). The false-alarm rates of the proposed zero-watermarking technology and the direct graying-based method are compared in Figure 6. The direct graying-based method recognised two of the 16 photos incorrectly, believing their values to be below the warning line (the threshold), In contrast, the proposed approach produced only one false detection. Furthermore, the proposed algorithm's complexity was clearly larger than that of the direct graying-based method, indicating a high degree of division and a lower proclivity to underestimate the watermark detection. As a result, in terms of zero-watermark detection and false-alarm rate, the proposed zero-watermarking scheme's QFr-PHFMs-based method beats the direct graying-based method [17] and the single channel-based method [18].

Table 2. Experimental Results of Host Image Subjected to Geometric Attacks

Attacks	*PSNR*	*d*		
		Traditional direct grayscale method	Traditional single channel method	The proposed method
Rotation 20°	20.15	0.000032	0.0000023	0.0000008
Rotation 30°	19.24	0.000088	0.000072	0.000056
Rotation 65°	18.46	0.00029	0.00062	0.000078
Rotation 90°	19.11	0	0	0
Scaling factor:0.7	23.04	0.0099	0.0087	0.0042
Scaling factor:1.2	26.23	0.00042	0.00068	0.000058
Scaling factor:1.8	24.19	0.034	0.023	0.002
Scaling factor:2.5	22.57	0.09	0.053	0.012
Translation up to 20 pixels	17.23	0.00002	0.00001	0.0000019
Translation left to 20 pixels	16.78	0.00004	0.00005	0.0000025
Translation right to 40 pixels	18.22	0.00006	0.00009	0.0000034
Translation down to 40 pixels	19.18	0.00006	0.00009	0.0000032

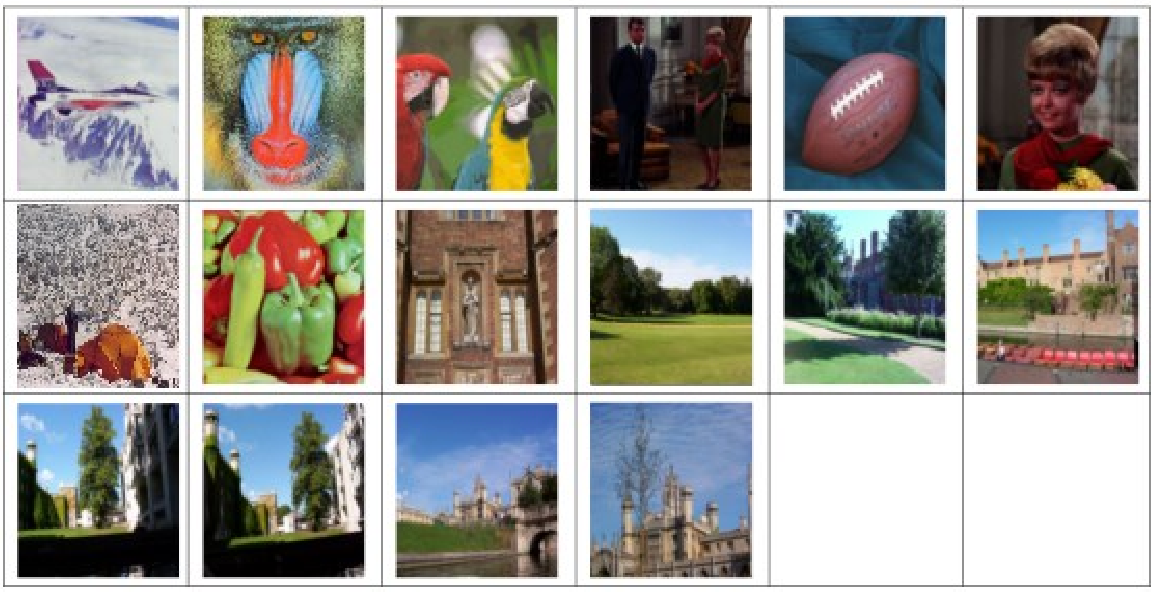

Figure 5. The 16 Color Images Selected for Checking the False-alarm Rate

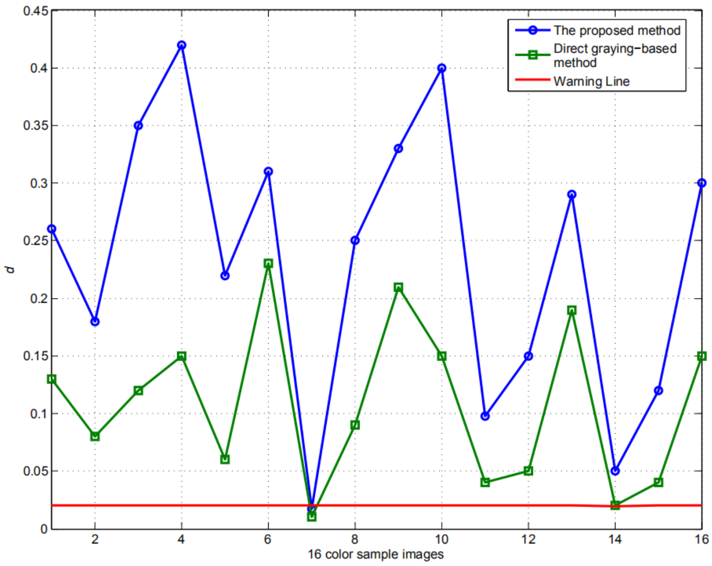

Figure 6. False-alarm Rates of Watermark Detection on the 16 Color Sample Images in Figure 5

VI.CONCLUSION

This research has proposed a new digital zero-watermarking technique for copyright protection of color images. The technique is based on wavelet transformation and QFr-PHFMs (Quaternion Fractional-order Polar Harmonic-Fourier Moments). The authors have performed experiments to evaluate the effectiveness of their proposed technique and found it to be successful and resistant to attacks that involve both noise interference and geometric transformations, particularly rotation. The results of the experiments indicate that the proposed color image zero-watermarking technology is practical and has great potential for use in copyright protection. The authors also express their intention to extend their feature-extraction approach to 3D zero-watermarking technology and other related fields to broaden the scope of the zero-watermarking methodology.

FUNDING

This work was supported by Weinan regional collaborative innovation development research project (Grant No. WXQY001-001 and WXQY002-007), Weinan Normal University Talent Fund Project (Grant No. 2021RC19) and Shaanxi Provincial Department of Education project (Grant No. 20JS044).

REFERENCES

[1] Z.Q.Xia, X.Y.Wang, X.X.Li, C.P.Wang, S.Unar, M.X.Wang and T.T.Zhao, "Efficient copyright protection for three CT images based on quaternion polar harmonic Fourier moments", Signal processing, 164(11):368-379(2019).

[2] K.M.Hosny, M.M.Darwish, M.M.Fouda, "New Color Image Zero-Watermarking Using Orthogonal Multi-Channel Fractional-Order Legendre-Fourier Moments", IEEE Access, 9(99):91209-91219,2021.

[3] Z.Yuan, D.Liu, X.Zhang, H.Wang and Q.Su," DCT-based color digital image blind watermarking method with variable steps", Multimedia Tools and Applications, 79(1):163-173,2020.

[4] X.Liu, Y.Wu, H.Zhang, J.Wu and L.Zhang,"Quaternion discrete fractional Krawtchouk transform and its application in color image encryption and watermarking",Signal Processing, 38(15): 173-178,2021.

[5] Q.Wen, T.Sun, S.Wang, "The concept and application of zero watermark. Acta electronica Sinica",31(2):214-216,2003.

[6] B.Ma, L.L.Chang, C.P.Wang, J.Li, L.Gang, Z.Q.Xia and X.Y.Wang, "Double Medical Images Zero-Watermarking Algorithm Based on the Chaotic System and Ternary Accurate Polar Complex Exponential Transform", Journal of Mathematical Imaging and Vision, 63(9):1160-1178, 2021.

[7] Z.Q.Xia, X.Y.Wang, C.P.Wang, C.X.Wang,B.Ma,Q.Li,M.X.Wang and T.T.Zhao,"A robust zero-watermarking algorithm for lossless

copyright protection of medical images",Applied Intelligence, 52(1):607-621,2022.

[8] T.F.Yang, J.F.Ma, Y.B.Miao, X.Wang, B.Xiao, B.He and Q.Meng, "Quaternion weighted spherical Bessel-Fourier moment and its invariant for color image reconstruction and object recognition",Information Sciences, 505:388-405,2019.

[9] B.J.Chen, H.Z.Shu, H.Zhang, G.Chen, C.Toumoulin, J.L.Dillenseger and L.M.Luo, "Quaternion Zernike moments and their invariants for color image analysis and object recognition", Signal Processing, 92:308-318,2012.

[10] K.M.Hosny, M.M.Darwish and T.Aboelenen, "New fractional-order Legendre-Fourier moments for pattern recognition applications", Pattern Recognition, 103:1-19,2020.

[11] B.Xiao, L.Li, Y.Li, W.Li, G Wang, "Image analysis by fractional-order orthogonal moments", Information Sciences, 382:135-149,2017.

[12] H.Q.Zhang, Z.M.Li, and Y.J. Liu, "Fractional Orthogonal Fourier-Mellin Moments for Pattern Recognition", Pattern Recognition. CCPR 2016, Communications in Computer and Information Science,662:766–778,2016.

[13] X.Y.Wang, W.Y.Li and H.Y.,Yang, "Quaternion polar complex exponential transform for invariant color image description", Applied Mathematics and Computation, 256(C):951-967,2015.

[14] B.J.Chen, H.Z.Shu, H.Zhang, G.Chen, C.Toumoulin, J.L.Dillenseger and L.M.Luo," Quaternion Zernike moments and their invariants for color image analysis and object recognition", Signal Processing, 92:308-318,2012.

[15] Z.H.Shao, H.Z.Shu, J.S.Wu, B.J.Chen and J.L.Coatrieux, "Quaternion Bessel–Fourier moments and their invariant descriptors for object reconstruction and recognition", Pattern Recognition,47(2):603-611,2014.

[16] Y.Lim, K.W.Ng, P.Naveen and S.C.Haw, "Emotion Recognition by Facial Expression and Voice: Review and Analysis", Journal of Informatics and Web Engineering, 1(2), 45-54,2022

[17] N.R.Jin, X.Q.Lv, Y.Gu,Y.Zhao and K.Liu "Blind watermarking algorithm for color image in Contourlet domain based on QR code and chaotic encryption", Packaging engineering, 38(15): 173-178,2017.

[18] Y.L.Hong, G.L.Qie, and H.W.Yu, "A contrast preserving color image graying algorithm based on two-step parametric subspace model", Frontiers of Information Technology & Electronic Engineering, (11): 102-116,2017.

[19] W.T.Chan, "Conditional Noise Filter for MRI Images with Revised Theory on Second-order Histograms",International Journal on Robotics, Automation and Sciences, 3, 25-32,2021